shRNA-induced knockdown of the *SPERT* gene inhibits proliferation and promotes apoptosis of human colorectal cancer RKO cells

LONG-ZHI ZHENG and SI-ZENG CHEN

Department of Gastrointestinal Surgery, The First Affiliated Hospital of Fujian Medical University,
Fuzhou, Fujian 350005, P.R. China

Abstract. Colorectal cancer is the third most common type of cancer and the fourth leading cause of cancer-related deaths worldwide. Although several genes have been identified to contribute to the pathogenesis of colorectal cancer, there are still many genes with unidentified functions in colorectal cancer. This study aimed to investigate the effect of shRNA-induced knockdown of the *SPERT* gene on the proliferation and apoptosis of human colorectal cancer RKO cells. *SPERT* was screened based on the TCGA dataset, and *SPERT* expression, cell growth, proliferation and apoptosis were detected in shSPERT- and shCtrl-transfected RKO cells. In addition, the SPERT-related biological pathways were detected using a PathScan® Signaling Antibody Array Kit. We detected lower SPERT expression in shSPERT-transfected RKO cells than in shCtrl-transfected cells at both the translational and transcriptional levels (P<0.05), and an MTT assay revealed a clear-cut decrease in the proliferation of shSPERT-transfected RKO cells relative to shCtrl-transfected RKO cells (P<0.01). A Caspase-Glo® 3/7 assay detected an increase in the caspase-3/7 activity and the number of apoptotic cells in the shSPERT-transfected RKO cells than in the shCtrl-transfected cells (P<0.01), and flow cytometry detected a higher apoptotic rate in the shSPERT-transfected RKO cells than in the shCtrl-transfected cells (20.65±0.26 vs. 5.93±0.06%, respectively, P<0.01). Elevated levels of phosphorylated p44/42 MAPK (ERK1/2), Akt, Bad, HSP27, p38 MARK and Chk2, and elevated PARP and caspase-3 expression levels were detected in shSPERT-transfected RKO cells compared with the shCtrl-transfected cells (P<0.05). The results of the current study demonstrated that knockdown of *SPERT* suppresses colorectal cancer cell growth and promotes apoptosis. *SPERT* may serve as an oncogene and may be a potential target for the treatment of colorectal cancer.

Introduction

Colorectal cancer (CRC) is the third most common type of cancer and the fourth leading cause of cancer-related deaths worldwide (1). Globally, ~1.2 million patients are newly diagnosed with CRC each year, and >600,000 succumb to this malignancy (2). At the time of their diagnosis, ~25% of patients with CRC already have distal liver and lung metastases, which often means that they have missed the opportunity for radical surgery. In addition, 35-55% of patients with CRC with disease progression may develop distal liver and lung metastases, resulting in a marked decline in survival (3-5). It is estimated that stage I patients with CRC have a 5-year survival rate of 80-90%, while patients with advanced disease have a 5-year survival rate of <10% (6). Early diagnosis and early treatment are therefore of great significance in improving the survival and prognosis of patients with CRC.

During the past several decades, there has been a stable but slow improvement in the prognosis of CRC (1). However, this could be greatly improved by precision medicine, which facilitates the improvement of disease diagnosis and the development of novel treatments, and helps select the optimal treatment strategy for CRC based on gene mutation detection (7). Based on analyses of cohorts comprised of twins from Sweden, Denmark and Finland, heritable factors are thought to contribute ~35% to CRC (8). To date, a number of genes (including *APC*, *p53* and *KRAS*) have been identified to be involved in the pathogenesis of CRC; however, there is still a large number of unidentified genes associated with the pathogenesis of CRC (9,10). Although several new hereditary CRC susceptibility genes have been identified, including DNA repair genes, DNA replication genes and genes related to the maintenance of genome stability (11), there is still no compelling evidence to support candidate genes for routine genetic diagnosis (12). Since the development of most CRC cases cannot be explained by known genes, the identification of CRC susceptibility genes is a high priority and is urgently needed.

Correspondence to: Dr Si-Zeng Chen, Department of Gastrointestinal Surgery, The First Affiliated Hospital of Fujian Medical University, 20 Chazhong Road, Fuzhou, Fujian 350005, P.R. China
E-mail: chensz04871@hotmail.com

As a comprehensive and coordinated effort to accelerate our understanding of the molecular basis of cancer, The Cancer Genome Atlas (TCGA) has generated comprehensive, multi-dimensional maps of the key genomic changes in multiple cancer types (13). In the present study, we screened a gene that has been shown to be differentially expressed in the development and progression of CRC, Spermatid-associated (*SPERT*), based on the TCGA dataset. Subsequently, we examined the effect of *SPERT* knockdown on the proliferation and apoptosis of the human CRC cell line RKO, and explored the mechanisms underlying these effects.

Materials and methods

Screening of target genes and evaluation of correlations between gene expression and clinicopathological characteristics. The TCGA dataset contains colon adenocarcinoma (COAD) and rectum adenocarcinoma (READ) data. When we analyzed the difference between cancer and peri-cancer expression for candidate gene screening, we selected paired samples from RNA-sequencing (RNA-Seq) and RNA-Seq Version 2 (RNA-SeqV2) to analyze the data (50 pairs). There were 41 pairs of colon cancer samples with pathological information and 9 pairs of rectal cancer samples with pathological information. For each gene symbol, the transcript with the highest expression was used for analysis (original reads >50), and transcripts were normalized with the Trimmed Mean of M-values (TMM) method (14). The following criteria were used for the screening of candidate genes: i) genes that have already been reported to be involved in CRC were excluded; ii) multi-transmembrane protein genes were excluded, because multiple transmembrane proteins generally have large molecular weights that are not easy to perform gene manipulation (e.g., knocked down or overexpressed), and most transmembrane proteins play the role of signal transmission and transduction; iii) genes with undefined annotations (such as open reading frames) were excluded; iv) genes with >100 publications in PubMed were excluded intended to ensure the originality and innovation of the genes we have screened. In order to render the analysis data more convincing, the range of analysis was extended to 624 RNA-Seq samples of colorectal cancer from the TCGA dataset after obtaining the differentially expressed *SPERT* gene in pairs of samples, to further analyze the difference of *SPERT* gene expression in different pathological stages of colorectal cancer.

Construction of shRNA lentiviral vectors. According to the RNA interference (RNAi) sequence, multiple RNAi target sequences (19-21 nucleotides in length) were designed, using the SPERT gene as a template. Following assessment by the design software, the sequence 5'-ACAAGATCCTAC AGGTCTT-3' was selected as an RNAi target (shSPERT): Forward primer, 5'-TACTTCTCCCCATCCGCCTCC-3' and reverse primer, 5'-GCGACGTGGTCCTTCTTCACC-3'. The scramble sequence 5'-TTCTCCGAACGTGTCACGT-3' served as an RNAi negative control (shCtrl): Forward primer, 5'-CCATGATTCCTTCATATTTGC-3' and reverse primer, 5'-GTAATACGGTTATCCACGCG-3'. The shRNA lentiviral vector targeting the SPERT gene (LV-SPERT-RNAi) and the

control lentiviral vector (LV-shRNA-NC) were constructed and packaged by Shanghai Genechem Co., Ltd. (Shanghai, China). The lentiviral vector contained a GFP open reading frame that could quickly and directly display the efficiency of lentiviral infection, which helped us to judge the expression of exogenous knockdown sequences in cultured cells. In addition, there was also a FLAG-tag which could be recognized by the Anti-Flag antibody, so it was convenient to detect and identify the target protein containing FLAG by western blotting.

Detection of SPERT expression in CRC cell lines by RT-qPCR. The human CRC cell lines RKO, SW480 and HCT116 were purchased from the Cell Bank of the Chinese Academy of Sciences (Shanghai, China), and were screened to determine *SPERT* expression. Total RNA was isolated from cells using TRIzol® reagent (Shanghai Pufei Biotech Co., Ltd., Shanghai, China) and reverse-transcribed into cDNA. *SPERT* gene expression (forward primer, 5'-TACTTCTCCCCATCCGCC TCC-3' and reverse primer, 5'-GCGACGTGGTCCTTCTTC ACC-3') was quantified in these three cells lines using a Roche LightCycler® 480 Real-Time PCR platform (Roche Diagnostics, Indianapolis, IN, USA) with 40 cycles at 95℃ for 5 sec and at 60℃ for 30 sec, while *GAPDH* (forward primer, 5'-TGACTTCAACAGCGACACCCA-3' and reverse primer, 5'-CACCCTGTTGCTGTAGCCAAA-3') served as the internal control. The relative quantity was calculated using the $2^{-\Delta\Delta Cq}$ method. Detection of *SPERT* expression was repeated in triplicate in each cell line. Of the three cell lines, the cell line expressing the highest level of *SPERT* was selected for use in further experiments.

The same RT-qPCR method was used to quantify *SPERT* mRNA levels after transfection of the chosen cell line, RKO, with the shRNA lentiviral constructs (as described below).

RKO cell culture and transfection. Human CRC RKO cells were incubated in RPMI-1640 medium (Beyotime Institute of Biotechnology, Shanghai, China) supplemented with 10% fetal bovine serum (Ausbian, Adelaide, Australia) at 37℃ in an atmosphere of 5% CO_2. Log-phase cells were digested with trypsin (Sangon Biotech Co., Ltd., Shanghai, China), and prepared as cell suspensions with complete DMEM (Corning Life Sciences, Manassas, VA, USA) at a density of $3x10^4$-$5x10^4$ cells/ml. Cells were then seeded into culture plates and grown until they reached 15-30% confluence. Subsequently, the cells were transfected with shSPERT or shCtrl at a multiplicity of infection (MOI) of 10, in the presence of Lipofectamine® 2000 reagent (Invitrogen; Thermo Fisher Scientific, Inc., Carlsbad, CA, USA). The medium was changed to RPMI-1640 at 8-12 h post-transfection, and the target gene expression was observed under an Olympus IX71 inverted fluorescence microscope (Olympus, Tokyo, Japan) at 72 h post-transfection.

Western blot analysis. At 48 h post-transfection, total protein was extracted using RIPA lysis buffer and quantified using a BCA protein assay kit (both from Beyotime Institute of Biotechnology). Total protein was then separated by 10% SDS-PAGE, and transferred to PVDF membranes (EMD Millipore, Bedford, MA, USA), which were blocked and incubated at 4℃ overnight. The blots were then incubated

with mouse anti-FLAG monoclonal antibodies (1:2,000 dilution; cat. no. F1804; Sigma-Aldrich Trading Co. Ltd., Shanghai, China), washed three times (10 min each) with TBST, incubated with the secondary antibody (goat anti-mouse IgG; dilution, 1:2,000; cat. no. sc-2005; Santa Cruz Biotechnology, Co., Ltd., Shanghai, China) for 1 h, and washed three times (10 min each) with TBST. The membranes were viewed with an Odyssey fluorescence imaging system (LI-COR Biosciences, Lincoln, NE, USA), and immunoreactive protein bands were visualized with the Pierce™ ECL Western Blotting Substrate (Pierce, Rockford, IL, USA). ImageJ (version 1.46 release; National Institutes of Health, Bethesda, MD, USA) software was used for quantification of the western blots.

Celigo-based cell-counting and viability assay. Log-phase cells were digested with trypsin, resuspended in complete DMEM and counted. Cells were then seeded into cell culture plates at a density of 2,000 cells/well in a 100-μl system, and three replicate wells were established for each group. Cells were incubated at 37˚C in an atmosphere of 5% CO_2. Commencing at day 2 post-seeding, the cells were counted on a Celigo® Image Cytometer (Nexcelom Bioscience, Lawrence, MA, USA) daily for 3-5 successive days. The 5-day cell growth curve was plotted.

MTT assay. Log-phase cells were digested with trypsin, resuspended in complete DMEM and counted. Cells were then seeded into cell culture plates, and three replicate wells were established for each group. Cells were incubated at 37˚C in an atmosphere of 5% CO_2. At day 2 post-seeding, 20 μl MTT solution (5 mg/ml; GenView Corp., Houston, TX, USA) was added to each well and incubated for 4 h, before the culture solution was completely removed, leaving the formazan crystals on the bottom of the well. Subsequently, 100 μl DMSO (Shanghai Shiyi Chemicals Reagent Co., Ltd., Shanghai, China) was added to dissolve the formazan crystals. Following vibration for 2-5 min, the optical density (OD) was measured at 490 nm using a Tecan Infinite M200 Pro Microplate Reader (Tecan Group, Ltd., Männedorf, Switzerland).

Caspase-Glo® 3/7 assay. Cells were seeded into 96-well plates, and incubated at 37˚C with 5% CO_2 for 3-5 days. Following cell counting, the cell density was adjusted to 1x10^4 cells/ml at room temperature. shSPERT- and shCtrl-transfected cells were transferred to a new 96-well plate, with 100 μl medium/well. Wells containing blank medium served as the negative controls. Subsequently, 100 μl of Caspase-Glo reagent (Promega Corp., Madison, WI, USA) was added to each well, and the well content was gently mixed with a plate shaker at 100-200 x g/min for 30 min. Following incubation at 18-22˚C for 0.5-3 h, the signal intensity was measured.

Flow cytometry. Log-phase cells were harvested, digested with trypsin, and resuspended in complete DMEM. The cell suspension and supernatant were then transferred to a 5-ml centrifuge tube and centrifuged at 300 x g/min for 5 min. Three replicate wells were assigned for each group (≥5x10^5 cells). The supernatant was then discarded, and the sediment was washed in 4˚C precooled D-Hanks' Balanced Salt Solution (pH 7.2-7.4). Subsequently, the cells were washed with 1X binding buffer and centrifuged at 300 x g/min for 3 min. The supernatant was discarded, and the sediment was resuspended in 200 μl of 1X binding buffer, and stained with 10 μl of Annexin V-APC (eBioscience, San Diego, CA, USA) at room temperature in darkness for 10-15 min. To each tube, 500 μl of 1X binding buffer was added, and the cells were then subjected to flow cytometry. All measurements were repeated in triplicate.

Detection of SPERT-related biological pathways. SPERT-related biological pathways were detected with the PathScan® Signaling Antibody Array Kit (Cell Signaling Technology, Inc., Danvers, MA, USA) following the manufacturer's instructions. Briefly, the cells were lysed, and incubated in 75 μl of 1X antibody mixture on a horizontal shaker for 1 h. The antibody mixture was removed, and the cells were washed four times with 1X wash buffer on a horizontal shaker (5 min each time). Then, the cells were incubated in 75 μl of 1X HRP-conjugated streptavidin on a horizontal shaker for 0.5 h. Following removal of HRP-conjugated streptavidin, the cells were washed four times with 1X wash buffer on a horizontal shaker (5 min each time). Finally, the cell slides were immersed in 1X wash buffer, visualized and analyzed. Cell slides were immersed in 1X washing buffer. Exposure buffer was formulated with 9 ml ddH$_2$0, 0.5 ml LumiGLO (Cell Signaling Technology, Danvers, USA) and 0.5 ml peroxide, and the cell slides were incubated with exposure buffer, then exposed within 1-2 sec using a visualization system (Clinx ChemiScope 5300; Clinx Science Instruments, Co., Ltd., Shanghai, China). The resulting images were analyzed using the visualization system aforementioned, and raw data were further analyzed manually.

Statistical analysis. All measurement data are presented as the mean ± standard deviation (SD). Differences in the means between groups were tested for statistical significance with the Student's t-test, and comparison of proportions was conducted with a Chi-square test. The association of *SPERT* expression with clinicopathological characteristics was examined with a Mann-Whitney U test. All statistical analyses were performed using SPSS statistical software version 17.0 (SPSS, Inc., Chicago, IL, USA), and a P-value of <0.05 was considered to indicate a statistically significant difference.

Results

Associations of SPERT expression with clinicopathological characteristics. All data were obtained from highly reliable genetic disease databases, and the gene list was finally obtained following random condensation (Table I). In fact, we screened ~6,000 disease-related genes in different tumor types, but to ensure the originality and innovation of the candidate genes, we selected the gene *SPERT* through the four screening conditions aforementioned. We first analyzed high-throughput RNA-sequencing data of the colon adenocarcinoma (COAD) and rectal adenocarcinoma (READ) cohorts of TCGA, and found that *SPERT* expression was significantly increased in CRC tissues compared with peri-cancer tissues (P<0.0001) (Table II and Fig. 1). Then, we analyzed the relationship between *SPERT* expression and various

Table I. Gene list for analysis based on The Cancer Genome Atlas dataset.

Gene ID	Gene name	No. of transcripts	Publications in PubMed	Novoseek disease relationships for the gene	MalaCards disease relationships for the gene
220082	*SPERT*	3	13	0	0

Table II. *SPERT* expression in colorectal cancer and peri-cancer specimens in The Cancer Genome Atlas dataset.

				No. of samples			
ID	Gene symbol	FC	P-value	Total	With unchanged *SPERT* expression	With upregulated *SPERT* expression	With downregulated *SPERT* expression
220082	*SPERT*	100.975	2.94E-56	50	5	45	0

Fold-change (FC) is calculated as SPERT expression in colorectal cancer specimens divided by SPERT expression in peri-cancer specimens.
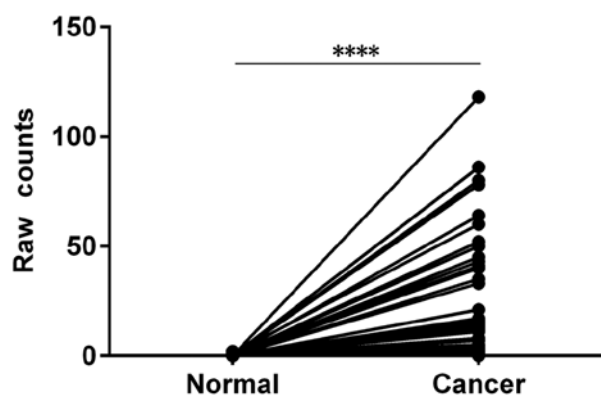
Figure 1. Significantly higher *SPERT* expression was detected in colorectal cancer specimens than in peri-cancer specimens (****P<0.0001).
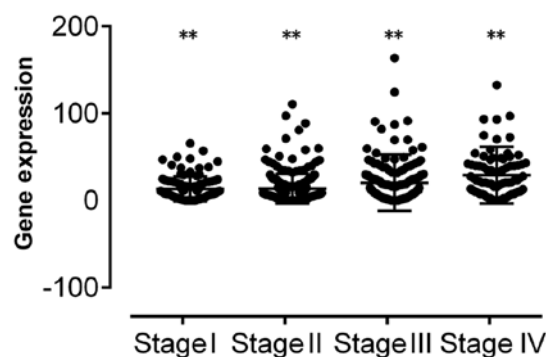
Figure 2. Associations between *SPERT* expression and various clinicopathological features in human colorectal cancer patients (**P<0.01).
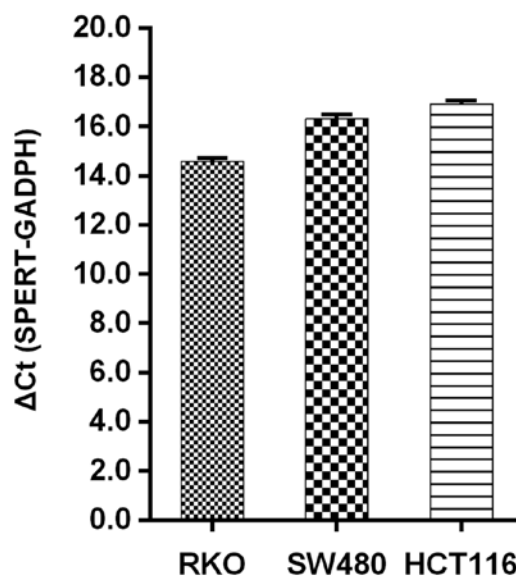

Figure 3. *SPERT* mRNA levels in three human colorectal cancer cell lines (RKO, SW480 and HCT116). The expression of *SPERT* mRNA was measured by RT-qPCR in the indicated cell lines. The constitutively expressed GAPDH gene was used as an internal control. ΔCt=Ct value of the target gene-Ct value of the internal reference gene. Cells with a higher ΔCt value express a lower level of the target gene. ΔCt ≤12 indicates high expression; 12< ΔCt <16 indicates moderate expression; ΔCt ≥16 indicates low expression.

SPERT expression in various human CRC cell lines. In order to fully demonstrate the effect of *SPERT* on CRC cells, we determined the cell line with the highest content of *SPERT* and selected this for use in subsequent experiments. RT-qPCR was used to quantify *SPERT* expression in the different cell lines (RKO, SW480 and HCT116 cells), and the results revealed that *SPERT* was most prominent in RKO cells, as revealed in Fig. 3. Therefore, RKO cells were selected for the subsequent experiments.

clinicopathological parameters of patients with CRC. The Mann-Whitney U test revealed that *SPERT* expression was associated with N, M and pathological stages in patients with CRC (all P<0.01) (Table III and Fig. 2).

Table III. Associations of *SPERT* expression with clinicopathological features in human colorectal cancer patients.

Clinicopathological features	SPERT expression, n		Total, n	P-value
	Low	High		
N				
N0	197	155	352	<0.001
N1/2	110	155	265	
Total	307	310	617	
M				
M0	243	215	458	<0.001
M1	27	61	88	
Total	270	276	546	
Pathological stage				
Stage I	56	49	105	0.001
Stage II	131	98	229	
Stage III	87	92	179	
Stage IV	28	62	90	
Total	302	301	603	

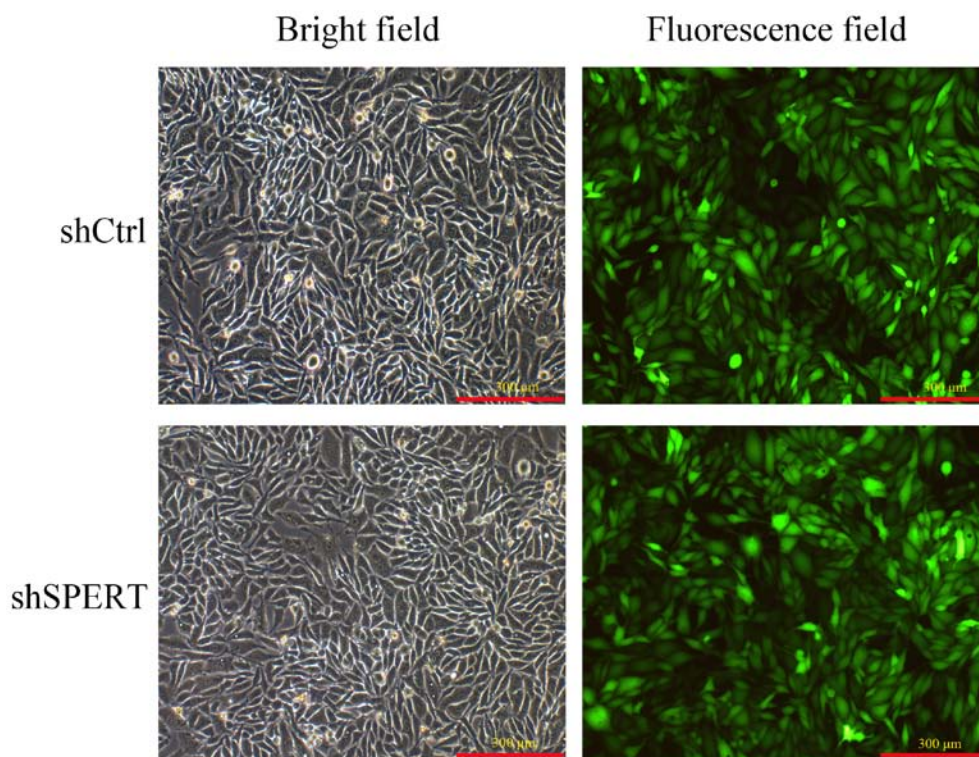N, local lymph node involvement; M, distal metastasis.

Figure 4. RKO cells were examined by fluorescence microscopy and light microscopy at the 72 h after transfection with the LV-SPERT-RNAi or LV-shRNA-NC (magnification, x100). >80% of the RKO cells expressed GFP.

SPERT expression following shRNA transfection. Fluorescence microscopy revealed that >80% of RKO cells were successfully infected with LV-SPERT-RNAi or LV-shRNA-NC at 72 h post-transfection, indicating a high success rate of lentiviral vector infection (Fig. 4). RT-qPCR detected decreased *SPERT* mRNA expression in shSPERT-transfected RKO cells than in shCtrl-transfected cells (0.437 ± 0.040 vs. 1.001 ± 0.046, respectively, P<0.01), and the transfection efficiency was 90.3% (Fig. 5A). Consistently, western blotting detected a reduction of $82.25 \pm 0.25\%$ in SPERT expression in the shSPERT-transfected RKO cells than in the shCtrl-transfected cells (P<0.01) (Fig. 5B and C). These results confirmed that
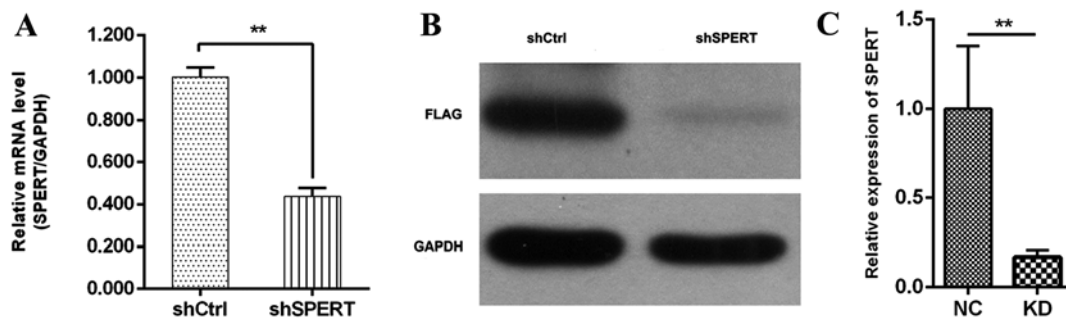
Figure 5. Confirmation of *SPERT* knockdown in RKO cells. (A) mRNA expression of *SPERT* in the shSPERT and shCtrl groups. *SPERT* mRNA levels decreased significantly after SPERT knockdown (**P<0.01). (B and C) Western blot analysis of SPERT protein levels in the NC and experimental groups (**P<0.01). GAPDH was used as a loading control.

RNAi could effectively reduce the endogenous expression of the target gene.

Effect of SPERT knockdown on RKO cell growth and proliferation. shSPERT-transfected RKO cells exhibited a decline in number on days 1-5 post-transfection, while the number of shCtrl-transfected cells increased, indicating that shRNA-induced knockdown of *SPERT* inhibited RKO cell proliferation (Fig. 6A and B). The MTT assay revealed a clear decrease in the proliferation of shSPERT-transfected RKO cells relative to shCtrl-transfected RKO cells (P<0.01), demonstrating that shRNA-induced knockdown of *SPERT* suppressed RKO cell proliferation (Fig. 6C).

Effect of SPERT knockdown on RKO cell apoptosis. The Caspase-Glo 3/7 assay detected an increase in the caspase-3/7 activity and the number of apoptotic cells in the shSPERT-transfected RKO cells than in the shCtrl-transfected cells (P<0.05) (Fig. 7C). Additionally, flow cytometry detected a higher apoptotic rate in the shSPERT-transfected RKO cells than in the shCtrl-transfected cells (20.65±0.26 vs. 5.93±0.06%, respectively, P<0.05) (Fig. 7A and B). These findings demonstrated that shRNA-induced knockdown of *SPERT* promoted RKO cell apoptosis.

SPERT-related biological pathways. To evaluate the SPERT-associated biological pathways, we used the PathScan® Signaling Antibody Array Kit from Cell Signaling Technology. The PathScan Stress and Apoptosis Signaling Antibody Array Kit (Chemiluminescent Readout) uses glass slides as the planar surface and is based upon the sandwich immunoassay principle. The array kit allows for the simultaneous detection of 19 signaling molecules that are involved in the regulation of the stress response and apoptosis. Target-specific capture antibodies are spotted in duplicate on nitrocellulose-coated glass slides. Each kit contains two slides allowing for the interrogation of 32 different samples and the generation of 608 data points in a single experiment. As shown in Fig. 8, the levels of phosphorylated p44/42 MAPK (ERK1/2), Akt, Bad, HSP27, p38 MARK and Chk2, as well as PARP and caspase-3 expression were elevated in shSPERT-transfected RKO cells compared with shCtrl-transfected cells (P<0.05, P<0.01), indicating that shRNA-induced knockdown of *SPERT* may suppress RKO cell proliferation and promote cell apoptosis via these proteins.

Discussion

CRC is one of the most common gastrointestinal cancers (1). Currently, surgery remains the primary treatment for CRC (15), and neoadjuvant and adjuvant radiochemotherapy have been shown to be effective in preventing post-surgical recurrence and improving the survival rate in patients with CRC (16,17). In addition, the introduction of targeted therapy has been shown to increase the median survival time from 3.6-6 to 24-28 months in patients with metastatic CRC (18-20).

CRC is a genetically heterogeneous disease (21). To date, the roles of APC, p53 and KRAS in the pathogenesis of CRC have been demonstrated; however, the contribution of other genes to the pathogenesis of CRC remains unclear (9,10). Systems biology studies have shown gene instability, microsatellite instability and methylation abnormalities in CRC (22). However, TCGA datasets provide valuable bases for clinical diagnosis, treatment and precision medicine for CRC (23-25).

In this study, the colon adenocarcinoma (COAD) and rectum adenocarcinoma (READ) datasets in the TCGA were used, and RNA-Seq and RNA-SeqV2 were employed to analyze gene expression in paired COAD and READ samples. *SPERT* was selected from the screening. There was a significant difference in *SPERT* expression between cancer and peri-cancer specimens in patients with CRC, and *SPERT* gene expression was significantly associated with lymph node metastasis, distal metastasis and pathological stages. Our data indicated that *SPERT* was involved in the progression of CRC, and may serve as an indicator for clinicopathological staging in patients with CRC.

In the present study, knockdown of *SPERT* was found to suppress human CRC RKO cell proliferation and promote cell apoptosis. It is therefore hypothesized that *SPERT* overexpression may be involved in the development, progression and metastasis of CRC. *SPERT*, which is located on human chromosome 13q14.13, encodes the SPERT protein (also known as CBY2 and Nurit), which contains 338 amino acids and has a molecular weight of 51,570 Da. SPERT belongs to the Chibby protein family and has a quaternary structure of homodimers. It is a highly conserved gene in mammals, it is expressed in humans, Rhesus monkeys, mice and rats, but it is not expressed in *Drosophila melanogaster* or *Caenorhabditis elegans* (26). However, the function of the SPERT protein has remained unknown until now. It is reported that the SPERT protein
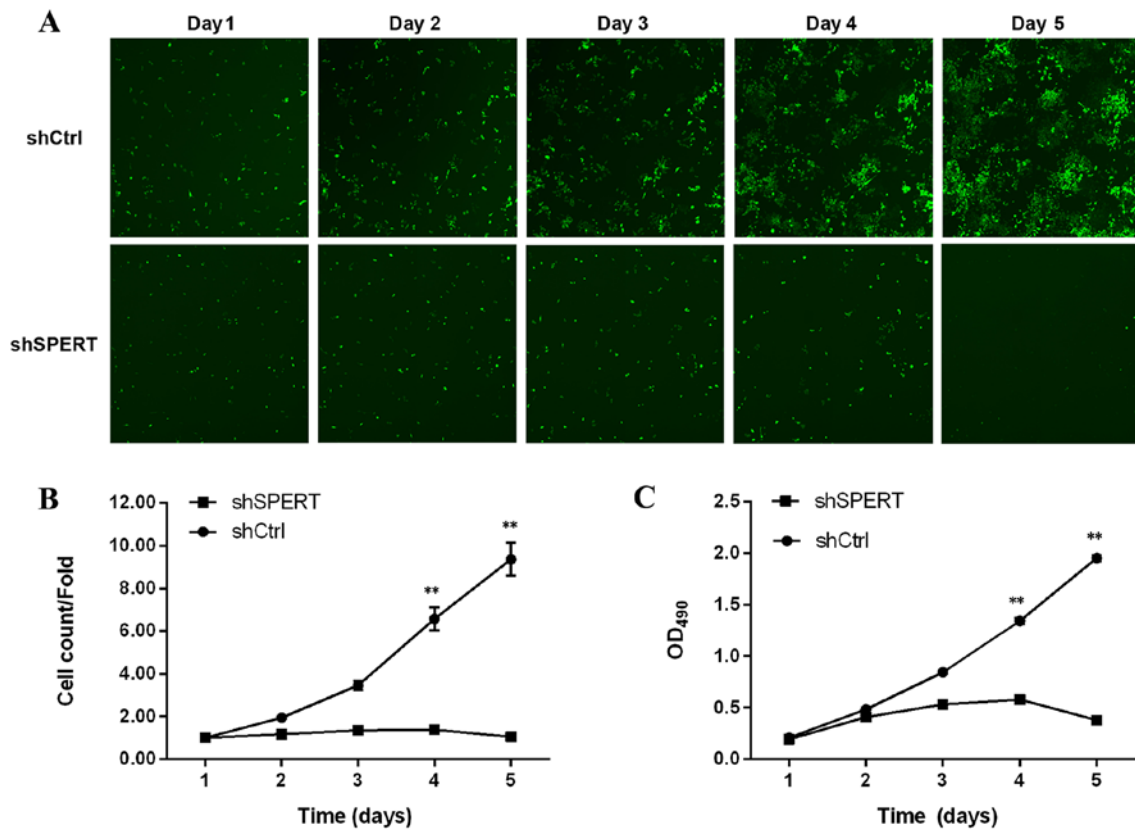
Figure 6. (A and B) Growth and (C) proliferation of shSPERT- and shCtrl-transfected RKO cells. (A) High-content cell-imaging assays were applied to acquire raw images (unprocessed by software algorithm) of cell growth. (B) Celigo analysis of cell proliferation in the shSPERT and shCtrl groups (**P<0.01). (C) MTT analysis of cell proliferation in the shSPERT and shCtrl groups (**P<0.01).
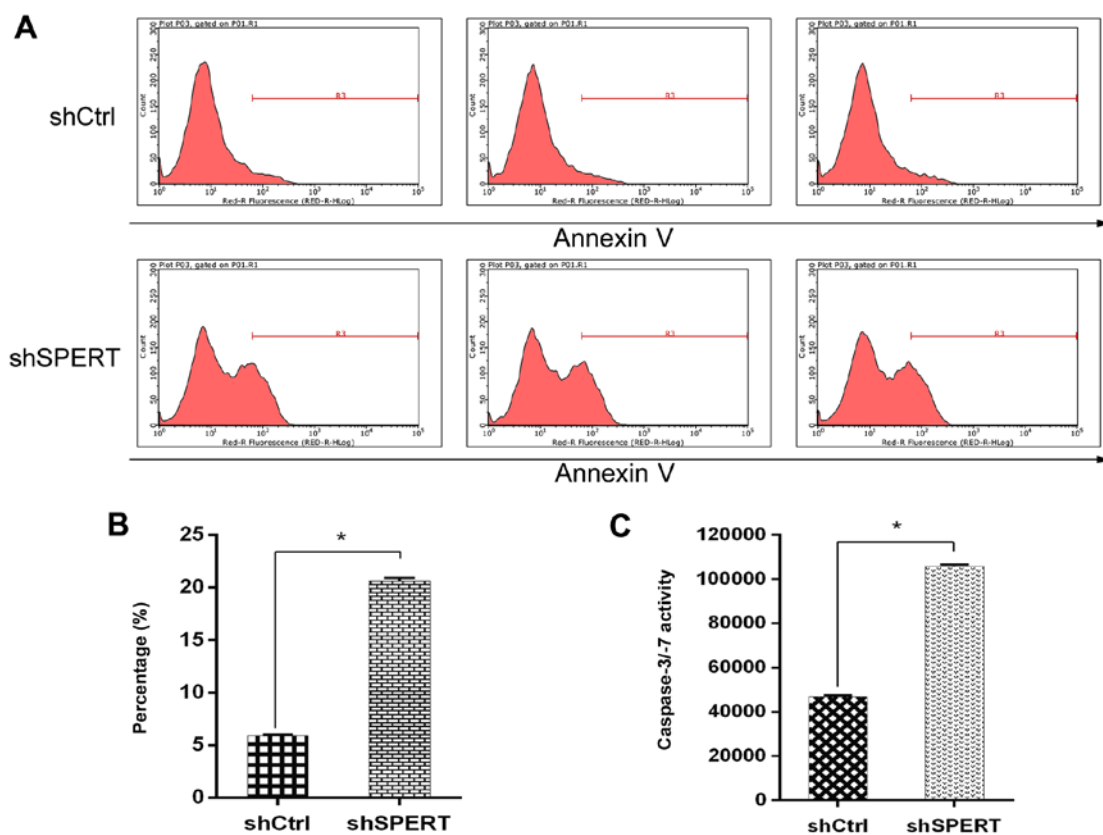

Figure 7. Knockdown of *SPERT* in RKO cells increases apoptosis. (A and B) Cell death was determined by Annexin V staining and flow cytometry. (C) Caspase-Glo® 3/7 Assay of the caspase-3 and -7 activation in the shSPERT and shCtrl groups. shSPERT cultures exhibited a significant increase in apoptosis compared with the shCtrl group (*P<0.05).
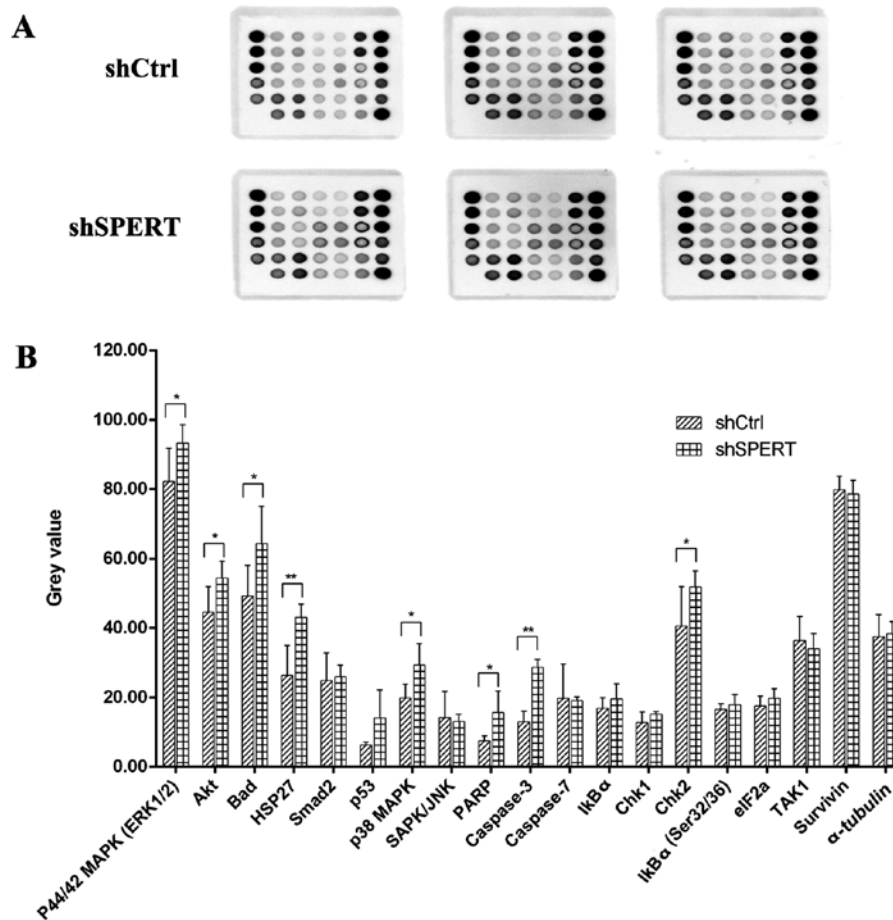
Figure 8. Mechanisms underlying the functions of SPERT in human colorectal cancer RKO cells. (A) Cell extracts were prepared and analyzed using the PathScan® Stress and Apoptosis Signaling Antibody Array Kit (Chemiluminescent Readout) (#12856). Images were acquired by briefly exposing the slide to standard chemiluminescent film. (B) PathScan detected stress and apoptosis signaling pathway-related genes (*P<0.05, **P<0.01 vs. shCtrl).

contains a leucine zipper motif and two coiled-coil regions, and the leucine zipper motif is involved in homodimerization or oligomerization, which is associated with the regulation of oncogene expression (27). It is known that SPERT proteins may form dimers in mice, and the C-terminal coiled-coil domain mediates protein dimerization, which may link with Nek1 kinase (26,28). Nek1, a member of the NIMA-related kinase family, is aberrantly expressed in multiple cancer types, and aberrant Nek1 expression was reported to cause abnormal regulation of the entire cell cycle and abnormal cell proliferation, thereby resulting in cancer development and progression (29,30). Further studies to examine the interplay between the SPERT protein and Nek1 appear justified.

To date, the exact role of SPERT in CRC remains unclear. In this study, the PathScan® Signaling Antibody Array Kit was employed to detect changes in key signaling molecules involved in stress and apoptosis signaling pathways. Our findings revealed upregulation of phosphorylated p44/42 MAPK (ERK1/2), Akt, Bad, HSP27, p38 MARK and Chk2, in addition to elevated PARP and Caspase-3 expression in shSPERT-transfected RKO cells, indicating that these proteins are involved in the progression of CRC, in which MAPK and PI3K/Akt signaling plays a predominant role. Bad is the downstream target of the MAPK and PI3K/Akt signaling pathways. MAPK regulates the function of the proapoptotic protein Bad

through the phosphorylation of serine 112, while PI3K/Akt regulates its function by phosphorylation of serine 136. The dissociation of phosphorylated Bad from anti-apoptotic factor Bcl-2 leads to an increase in the activity of free Bcl-2, which inhibits apoptosis (31). Caspase-3 and HSP27 are the downstream target proteins of the p38 MAPK/HSP27 signaling pathway, and the most important substrate of caspase-3 is the poly(ADP-ribose) polymerase PARP. PARP cleavage is closely related to cell apoptosis and is one of the markers of cell apoptosis and caspase activation (32). MAP kinase cascades mediate Hsp27 phosphorylation, MAPKAPK2 and MAPKAPK3 regulate the function of the *heat shock protein 27 (HSP27)* by phosphorylating it on distinct sites, Ser-15, Ser-78 and Ser-82. Downstream, HSP27 also blocks the activation of caspase-9 and subsequent activation of caspase-3, thereby inhibiting the remaining of the proteolytic caspase cascade (33,34).

It has been revealed that both the MAPK and PI3K/Akt pathways, which are associated with cancer initiation and progression, serve critical roles in CRC progression and greatly contribute to intestinal epithelial cell differentiation (35-39). *Ras* mutations have been detected in 35-45% of patients with CRC (40-43), while 9-11% of patients with CRC harbor *BRAF* mutations (44-46). *KRAS* and *BRAF* have been demonstrated to contribute to CRC progression (43,45). ERK1 and ERK2, which are located downstream of the

Ras oncogene protein, bind to cell-surface receptor tyrosine kinases and G-protein-coupled receptors, resulting in Ras and BRAF activation (47) and subsequent MEK1/MEK2 and ERK1/ERK2 phosphorylation (48). The Ras/Raf/MEK/ERK cascade has been revealed to be involved in the mediation of cell growth signals, cell survival and cancer invasion (49), and is strongly associated with the differentiation, pathological stage and prognosis of cancers, which may be used to guide the selection of targeted drugs for use in clinical cancer therapies (50). Our findings revealed that knockdown of *SPERT* significantly increased the levels of phosphorylated p44/42 MAPK (ERK1/2) and p38 MAPK; this may explain why *SPERT* knockdown suppressed RKO cell proliferation and promoted cell apoptosis. Further studies are required to investigate the detailed mechanisms underlying the SPERT-mediated effects on the MAPK and PI3K/Akt signaling pathways.

In summary, the results of the present study demonstrated that *SPERT* expression was significantly upregulated in CRC specimens, and knockdown of *SPERT* suppressed CRC cell growth and promoted apoptosis via the MAPK and PI3K/Akt signaling pathways. *SPERT* may serve as an oncogene for CRC, and may be a promising biomarker for predicting the poor prognosis of CRC. In addition, *SPERT* may be a potential target for the treatment of CRC.

Acknowledgements

Not applicable.

Funding

Availability of data and materials

The datasets used during the present study are available from the corresponding author upon reasonable request.

Authors' contributions

SZC and LZZ conceived and designed the study. LZZ performed the experiments and wrote the paper. SZC reviewed and edited the manuscript. All authors read and approved the manuscript and agree to be accountable for all aspects of the research in ensuring that the accuracy or integrity of any part of the work are appropriately investigated and resolved.

Ethics approval and consent to participate

Not applicable.

Consent for publication

Not applicable.

Competing interests

The authors state that they have no competing interests.

References

1. Brenner H, Kloor M and Pox CP: Colorectal cancer. Lancet 383: 1490-1502, 2014.
2. GBD 2015 Mortality and Causes of Death Collaborators: Global, regional, and national life expectancy, all-cause mortality, and cause-specific mortality for 249 causes of death, 1980-2015: A systematic analysis for the Global Burden of disease study 2015. Lancet 388: 1459-1544, 2016.
3. Kelly C and Cassidy J: Chemotherapy in metastatic colorectal cancer. Surg Oncol 16: 65-70, 2007.
4. Bouche O, Conroy T, Michel P, Penna C and Tournigand C: Metastatic colorectal cancer. Gastroenterol Clin Biol 30: 2S30-2S42, 2006.
5. Yau T, Chan P, Ching Chan Y, Wong BC, Liang R and Epstein RJ: Current management of metastatic colorectal cancer-the evolving impact of targeted drug therapies. Aliment Pharmacol Ther 27: 997-1005, 2008.
6. Wilkes G and Hartshorn K: Clinical update: Colon, rectal, and anal cancers. Semin Oncol Nurs 28: e1-e22, 2012.
7. Tran NH, Cavalcante LL, Lubner SJ, Mulkerin DL, LoConte NK, Clipson L, Matkowskyj KA and Deming DA: Precision medicine in colorectal cancer: The molecular profile alters treatment strategies. Ther Adv Med Oncol 7: 252-262, 2015.
8. Lichtenstein P, Holm NV, Verkasalo PK, Iliadou A, Kaprio J, Koskenvuo M, Pukkala E, Skythe A and Hemminki K: Environmental and heritable factors in the causation of cancer-analyses of cohorts of twins from Sweden, Denmark, and Finland. N Engl J Med 343: 78-85, 2000.
9. Wood LD, Parsons DW, Jones S, Lin J, Sjöblom T, Leary RJ, Shen D, Boca SM, Barber T, Ptak J, et al: The genomic landscapes of human breast and colorectal cancers. Science 318: 1108-1113, 2007.
10. Sjöblom T, Jones S, Wood LD, Parsons DW, Lin J, Barber TD, Mandelker D, Leary RJ, Ptak J, Silliman N, et al: The consensus coding sequences of human breast and colorectal cancers. Science 314: 268-274, 2006.
11. Nassiri M, Kooshyar MM, Roudbar Z, Mahdavi M and Doosti M: Genes and SNPs associated with non-hereditary and hereditary colorectal cancer. Asian Pac J Cancer Prev 14: 5609-5614, 2013.
12. Hampel H: Genetic testing for hereditary colorectal cancer. Surg Oncol Clin N Am 18: 687-703, 2009.
13. Cancer Genome Atlas Research Network; Weinstein JN, Collisson EA, Mills GB, Shaw KR, Ozenberger BA, Ellrott K, Shmulevich I, Sander C and Stuart JM: The cancer genome atlas Pan-cancer analysis project. Nat Genet 45: 1113-1120, 2013.
14. Lin Y, Golovnina K, Chen ZX, Lee HN, Negron YL, Sultana H, Oliver B and Harbison ST: Comparison of normalization and differential expression analyses using RNA-Seq data from 726 individual *Drosophila melanogaster*. BMC Genomics 17: 28, 2016.
15. Coffey JC and Dockery P: Colorectal cancer: Surgery for colorectal cancer-standardization required. Nat Rev Gastroenterol Hepatol 13: 256-257, 2016.
16. Sauer R, Fietkau R, Wittekind C, Rödel C, Martus P, Hohenberger W, Tschmelitsch J, Sabitzer H, Karstens JH, Becker H, et al: Adjuvant vs. neoadjuvant radiochemotherapy for locally advanced rectal cancer: The German trial CAO/ARO/AIO-94. Colorectal Dis 5: 406-415, 2003.
17. Benson AB Rd: Should we consider adjuvant therapy for rectal cancer after neoadjuvant chemoradiotherapy? Clin Adv Hematol Oncol 14: 778-781, 2016.
18. Arnold D and Seufferlein T: Targeted treatments in colorectal cancer: State of the art and future perspectives. Gut 59: 838-858, 2010.
19. Seeber A and Gastl G: Targeted therapy of colorectal cancer. Oncol Res Treat 39: 796-802, 2016.
20. Pai SG and Fuloria J: Novel therapeutic agents in the treatment of metastatic colorectal cancer. World J Gastrointest Oncol 8: 99-104, 2016.
21. Lu YW, Zhang HF, Liang R, Xie ZR, Luo HY, Zeng YJ, Xu Y, Wang LM, Kong XY and Wang KH: Colorectal cancer genetic heterogeneity delineated by multi-region sequencing. PLoS One 11: e0152673, 2016.
22. Sonachalam M, Shen J, Huang H and Wu X: Systems biology approach to identify gene network signatures for colorectal cancer. Front Genet 3: 80, 2012.
23. Lee H, Palm J, Grimes SM and Ji HP: The cancer genome atlas clinical explorer: A web and mobile interface for identifying clinical-genomic driver associations. Genome Med 7: 112, 2015.

24. Wang Z, Jensen MA and Zenklusen JC: A practical guide to the cancer genome atlas (TCGA). Methods Mol Biol 1418: 111-141, 2016.
25. Hartman M, Loy EY, Ku CS and Chia KS: Molecular epidemiology and its current clinical use in cancer management. Lancet Oncol 11: 383-390, 2010.
26. Feige E, Chen A and Motro B: Nurit, a novel leucine-zipper protein, expressed uniquely in the spermatid flower-like structure. Mech Dev 117: 369-377, 2002.
27. Alber T: Structure of the leucine zipper. Curr Opin Genet Dev 2: 205-210, 1992.
28. Takemaru K, Yamaguchi S, Lee YS, Zhang Y, Carthew RW and Moon RT: Chibby, a nuclear beta-catenin-associated antagonist of the Wnt/Wingless pathway. Nature 422: 905-909, 2003.
29. Letwin K, Mizzen L, Motro B, Ben-David Y, Bernstein A and Pawson T: A mammalian dual specificity protein kinase, Nek1, is related to the NIMA cell cycle regulator and highly expressed in meiotic germ cells. EMBO J 11: 3521-3531, 1992.
30. Upadhya P, Birkenmeier EH, Birkenmeier CS and Barker JE: Mutations in a NIMA-related kinase gene, *Nek1*, cause pleiotropic effects including a progressive polycystic kidney disease in mice. Proc Natl Acad Sci USA 97: 217-221, 2000.
31. She QB, Solit DB, Ye Q, O'Reilly KE, Lobo J and Rosen N: The BAD protein integrates survival signaling by EGFR/MAPK and PI3K/Akt kinase pathways in PTEN-deficient tumor cells. Cancer Cell 8: 287-297, 2005.
32. Ivana Scovassi A and Diederich M: Modulation of poly(ADP-ribosylation) in apoptotic cells. Biochem Pharmacol 68: 1041-1047, 2004.
33. Bitar KN: HSP27 phosphorylation and interaction with actin-myosin in smooth muscle contraction. Am J Physiol Gastrointest Liver Physiol 282: G894-G903, 2002.
34. Bruey JM, Paul C, Fromentin A, Hilpert S, Arrigo AP, Solary E and Garrido C: Differential regulation of HSP27 oligomerization in tumor cells grown in vitro and in vivo. Oncogene 19: 4855-4863, 2000.
35. Fang JY and Richardson BC: The MAPK signalling pathways and colorectal cancer. Lancet Oncol 6: 322-327, 2005.
36. Miki H, Yamada H and Mitamura K: Involvement of p38 MAP kinase in apoptotic and proliferative alteration in human colorectal cancers. Anticancer Res 19: 5283-5291, 1999.
37. Abubaker J, Bavi P, Al-Harbi S, Ibrahim M, Siraj AK, Al-Sanea N, Abduljabbar A, Ashari LH, Alhomoud S, Al-Dayel F, *et al*: Clinicopathological analysis of colorectal cancers with PIK3CA mutations in Middle Eastern population. Oncogene 27: 3539-3545, 2008.
38. Ollikainen M, Gylling A, Puputti M, Nupponen NN, Abdel-Rahman WM, Butzow R and Peltomäki P: Patterns of *PIK3CA* alterations in familial colorectal and endometrial carcinoma. Int J Cancer 121: 915-920, 2007.
39. Taupin D and Podolsky DK: Mitogen-activated protein kinase activation regulates intestinal epithelial differentiation. Gastroenterology 116: 1072-1080, 1999.
40. De Roock W, Claes B, Bernasconi D, De Schutter J, Biesmans B, Fountzilas G, Kalogeras KT, Kotoula V, Papamichael D, Laurent-Puig P, *et al*: Effects of *KRAS*, *BRAF*, *NRAS*, and *PIK3CA* mutations on the efficacy of cetuximab plus chemotherapy in chemotherapy-refractory metastatic colorectal cancer: A retrospective consortium analysis. Lancet Oncol 11: 753-762, 2010.
41. Herreros-Villanueva M, Chen CC, Yuan SS, Liu TC and Er TK: *KRAS* mutations: Analytical considerations. Clin Chim Acta 431: 211-220, 2014.
42. Andreyev HJ, Norman AR, Cunningham D, Oates J, Dix BR, Iacopetta BJ, Young J, Walsh T, Ward R, Hawkins N, *et al*: Kirsten ras mutations in patients with colorectal cancer: The 'RASCAL II' study. Br J Cancer 85: 692-696, 2001.
43. Andreyev HJ, Norman AR, Cunningham D, Oates JR and Clarke PA: Kirsten ras mutations in patients with colorectal cancer: The multicenter 'RASCAL' study. J Natl Cancer Inst 90: 675-684, 1998.
44. Deng G, Bell I, Crawley S, Gum J, Terdiman JP, Allen BA, Truta B, Sleisenger MH and Kim YS: *BRAF* mutation is frequently present in sporadic colorectal cancer with methylated hMLH1, but not in hereditary nonpolyposis colorectal cancer. Clin Cancer Res 10: 191-195, 2004.
45. Davies H, Bignell GR, Cox C, Stephens P, Edkins S, Clegg S, Teague J, Woffendin H, Garnett MJ, Bottomley W, *et al*: Mutations of the *BRAF* gene in human cancer. Nature 417: 949-954, 2002.
46. Rajagopalan H, Bardelli A, Lengauer C, Kinzler KW, Vogelstein B and Velculescu VE: Tumorigenesis: *RAF/RAS* oncogenes and mismatch-repair status. Nature 418: 934, 2002.
47. Roskoski R Jr: ERK1/2 MAP kinases: Structure, function, and regulation. Pharmacol Res 66: 105-143, 2012.
48. Shama J, Garcia-Medina R, Pouysségur J and Vial E: Major contribution of MEK1 to the activation of ERK1/ERK2 and to the growth of LS174T colon carcinoma cells. Biochem Biophys Res Commun 372: 845-849, 2008.
49. Roberts PJ and Der CJ: Targeting the Raf-MEK-ERK mitogen-activated protein kinase cascade for the treatment of cancer. Oncogene 26: 3291-3310, 2007.
50. Hilger RA, Scheulen ME and Strumberg D: The Ras-Raf-MEK-ERK pathway in the treatment of cancer. Onkologie 25: 511-518, 2002.